Journal of Biotechnology 303 (2019) 16–24

Contents lists available at ScienceDirect

Journal of Biotechnology

journal homepage: www.elsevier.com/locate/jbiotec

In-vivo half-life and hypoglycemic bioactivity of a fusion protein of exenatide and elastin-based polypeptide from recombinant *Saccharomyces cerevisiae*

Su Jin Jung[a], Ngoc-Thanh Thi Nguyen[a], Sang Ah Lee[a], Sung Hwa Seo[b], Eui-Sung Choi[b], Hong Weon Lee[b], Gi Hun Seong[a,*], Ok Nam Bae[c], E.K. Lee[a,d,*]

[a] Department of Bionanotechnology, Graduate School, Hanyang University, Ansan, Gyeonggi-do, 15588, Republic of Korea
[b] Bio Process Engineering Center, KRIBB Ochang Branch Institute, Cheongju, Chungcheongbuk-do, 28116, Republic of Korea
[c] College of Pharmacy, Hanyang University, Ansan, Gyeonggi-do, 15588, Republic of Korea
[d] Immunoforge, Ltd., Seoul, 08826, Republic of Korea

ARTICLE INFO

Keywords:
Exenatide
Elastin-based polypeptide (EBP)
EBPylation
Half-life extension
Type 2 diabetes
Hypoglycemic efficacy

ABSTRACT

Exenatide (Ex) is a 39-amino acid peptide of glucagon-like peptide-1 (GLP-1) receptor agonist that was approved by the FDA in 2005 as a Type II diabetes treatment. It shows a 53% homology with GLP-1 but has an extended half-life (ca. 2.4 h) relative to GLP-1 (ca. 2–3 min). In this study, to further extend its *in vivo* half-life, we constructed a fusion protein (Ex-$(EBP)_{10}$-6xHis) using a biocompatible and inert elastin-based polypeptide (EBP) as a fusion partner. Valine was inserted into the guest position of the pentapeptide (VPGXG), no linker sequence was inserted in between the EBPs, and $(EBP)_{10}$-6xHis tag was attached to the C-terminus of exenatide. By using a recombinant *Saccharomyces cerevisiae* expression system, the fusion protein was expressed and secreted to the broth and purified by Ni-NTA affinity chromatography. Compared with the native exenatide, the physical half-life of the fusion protein was ca. 3.7-fold extended while approximately 72% of the in-vitro insulin secreting activity was maintained. However, the biological half-life measured by a glucose tolerance test (GTT) and the hypoglycemic test in mice was not significantly different from that of the native form. The effects of EBPylation on bioactivity and half-life of the fusion protein are similar to those of PEGylation. The result suggests that the bioactivity and half-life should be carefully balanced to obtain optimal fusion proteins. We expect that EBPylation using an optimal repeat number of EBP can be an alternative to chemical modification for therapeutic biobetters with extended half-life.

1. Introduction

Exenatide is a synthetic peptide of exendin-4 that is composed of 39 amino acids and has 53% structural homology to the glucagon-like peptide-1 (GLP-1), a peptide hormone produced in the intestinal epithelial cells stimulating insulin secretion and controlling blood glucose homeostasis (Eng et al., 1992). Exenatide has a relatively longer half-life (ca. 2.4 h) than GLP-1 (2–3 min) because of its resistance to DPP-IV (dipeptidyl peptidase-IV) protease which breaks down the N-terminus of GLP-1 (Mentlein et al., 1993; Parkes et al., 2001). Exenatide binds to the human GLP-1 receptor and enhances glucose-dependent insulin secretion, suppresses inappropriate pancreatic release of glucagon, promotes β-cell proliferation, and helps to slow down gastric emptying (Bunck et al., 2009). It was approved by the US Food and Drug Administration in 2005 as Type II diabetes therapeutics. However, exenatide should be injected subcutaneously twice a day for the continued efficacy, and this inconvenience has driven the development of a long-acting exenatide with an extended *in vivo* half-life to reduce the injection frequency (Zhou et al., 2009; Podust et al., 2016; Zhang et al., 2014; van Witteloostuijn et al., 2016).

The protein modification approach is frequently used to obtain 'biobetters' for improved functionalities and pharmacokinetic properties. Two types of protein modification have been developed. First, the chemical modification method chemically attaches a functional domain or material to a specific site on the protein surface through a bioconjugation technique. A good example is PEGylation (Harris and Chess, 2003). In PEGylation, the PEGylated protein, or a PEGylate, is generated by a covalent conjugation between a functional group of an

* Corresponding authors.
E-mail addresses: ghseong@hanyang.ac.kr (G.H. Seong), eklee@hanyang.ac.kr (E.K. Lee).

https://doi.org/10.1016/j.jbiotec.2019.06.304
Received 11 February 2019; Received in revised form 7 June 2019; Accepted 26 June 2019
Available online 03 July 2019
0168-1656/

activated polyethylene glycol (PEG), a generally regarded as safe (GRAS) substance, and a functional group of specific residues of a protein. In this case, however, additional efforts are required to change the gene of a target protein for site-specific PEGylation, such as substituting a specific amino acid residue with another residue or adding a specific residue at the terminus. In addition, post-PEGylation purification often requires several steps of cumbersome and delicate chromatographies resulting in a low recovery yield (Schellekens et al., 2013; Lee et al., 2007). Furthermore, activated PEG, which is an artificial polymer, is rather expensive and it has polydispersed molecular weight distribution, especially for higher molecular weight species

The second approach is a genetic modification of a target peptide/protein for a fusion protein with a functional domain attached as a fusion partner. In this case, since the fusion protein is expressed from the host cell, it is possible to guarantee the correct amino acid sequence and thus molecular weight. However, the partner domain itself may form a tertiary structure or cause a protein-protein interaction with a specific domain of the target protein, which could damage the physicochemical properties and biological functions of a target protein (Chuang et al., 2002). For example, human albumin or Fc fragment of antibodies (e.g., human IgGs) is often used as a fusion partner because of their neonatal Fc receptor (FcRn)-mediated recycling capability.

In this study, a genetic modification method using biocompatible and inert elastin-based polypeptides (EBP) as a fusion partner, namely EBPylation, was developed as a new half-life extension technology to overcome the disadvantages of the current chemical and genetic modifications. EBP_n (n = repeat number) are natural biopolymers consisting of a repeat sequence of a pentapeptide, VPGXG, where X can be any naturally occurring amino acid, except proline. Proline is excluded to render EBP a more unstructured helical conformation without specific structures. When $(EBP)_n$ is genetically attached to a target protein, it is possible to overcome the disadvantages of a chemical modification such as higher immunogenicity and lower stability. It has been widely studied as an interesting bionano material with inert, biocompatible, and thermo-responding characteristics (Floss et al., 2010).

However, most studies have focused on its temperature-dependent phase transition, i.e., sol-gel switching capability (Han et al., 2017) and those on applying EBPylation to half-life extension of a target protein are relatively scarce. Recently, a US patent was issued for a recombinant fusion protein between an elastic polypeptide and GLP-1 as a therapeutic agent with significantly extended half-life (Chilkoti, 2012). Also, a US biotech company, PhaseBio, Inc., reported a successful Phase IIa clinical study result, in which a 636 amino acid polypeptide comprising GLP-1 genetically fused to 120 ELP repeats significantly reduced mean glucose levels in humans over a 7 day period with minimal loss of glycemic control (Binder and Skerra, 2015).

EBPylated proteins are usually expressed in the cytoplasm of recombinant *E. coli* (Floss et al., 2010; Trabbic-Carlson et al., 2004; Hassouneh et al., 2012). In this study, however, we employed a recombinant *Saccharomyces cerevisiae* for the expression of EBPylated exenatide, since it is a generally recognized as a safe (GRAS) microorganism with an efficient protein secretory system. Since the protein is secreted into the broth, we could bypass the complicated cell disruption and the subsequent clarification processes and purify the fusion protein ($Ex\text{-}(EBP)_{10}$-6xHis) by a simple affinity chromatography. Functional characteristics such as *vivo* half-life and hypoglycemic bioactivity of the fusion protein were investigated and compared with those of the mono-PEGylated exenatide.

2. Materials and methods

2.1. Materials

Synthetic exendin-4 (exenatide) was obtained from CS Bio Co. (Menlo Park, CA, USA)and the gene of the fusion protein, EBPylated exenatide, i.e., $Ex\text{-}(EBP)_{10}$, was synthesized from Gen Script Inc. (Piscataway, NJ, USA). The restriction enzyme used for gene cloning was purchased from Takara Bio Inc. (Kusatsu, Shiga, Japan). DH5α competent cell (Real biotech Corporation, Taipei, Taiwan) was used as a strain for gene cloning in *E. coli*. We used the Y2805 strain of *S. cerevisiae* equipped with pYEGα vector for protein expression and MFα prepro secretion signal peptide gene (Choi et al., 1994).

The N-terminal amino acid sequence of the expressed protein was analyzed in the EMass Center (Seoul, Korea). Matrix assisted laser desorption/ionization time-of-flight (MALDI-TOF) mass spectrometry analysis was commissioned by the Korea Basic Science Research Institute (Ochang, Chungbuk, Korea). Other reagents were purchased from Sigma–Aldrich (St. Louis, Missouri, USA) and BD Biosciences (Franklin Lakes, NJ, USA).

2.2. Construction of recombinant $Ex\text{-}(EBP)_{10}$-6xHis expression plasmid

The exenatide with EBP was constructed inserting valine to the X amino acid position in the EBP (VPGXG) sequence. Ten repeats of EBP without a linker sequence, $(EBP)_{10}$, which has ca. 5 kD molecular weight, was fused at the C-terminus of the exenatide for $Ex\text{-}(EBP)_{10}$. To secrete the fusion protein into the medium, a MFα prepro secretion signal peptide was attached to the N-terminus, and for affinity purification 6x-His-tag was attached to the C-terminus by polymerase chain reaction (PCR) (Waters et al., 1988). This gene was cleaved with XbaI/SalI and ligated into the corresponding restriction sites in the pYEGα to place them under the control of the GAL 10 promoter and the GAL7 terminator for a galactose inducible expression system, resulting in the plasmid pYEGα-MFα prepro-$Ex\text{-}(EBP)_{10}$-6xHis. The amino acid sequence of the $Ex\text{-}(EBP)_{10}$ is: HGEGTFTSDLSKQMEEEQVRLFIEWLKNGGPSSGAPPPSVPGVGVPGVGVPGVGVPGVGVPGVGVPGVGVPGVGVPGVGVPGVG.

2.3. Yeast expression of $Ex\text{-}(EBP)_{10}$-6xHis

The plasmid was transformed into the *S. cerevisae* Y2805 strain using the LiAc/TE method (Hill et al., 1991), and the cells were plated on UD agar medium (yeast nitrogen base without amino acids6.7 g/L, Ura(-) DO supplement 0.77 g/L and glucose 20 g/L at pH 5.8) for the transformants selection. The selected colony was picked and cultivated in the UD medium, and then transferred to 500 ml of YPDG medium (yeast extract 10.0 g/L, peptone 20.0 g/L, glucose 10.0 g/L and galactose 10.0 g/L) in a 2 L shake flask for the recombinant protein expression at 30 °C for 48 h. The culture was centrifuged at 8000 rpm for 20 min to collect the culture broth supernatant, which was used as the crude source of the fusion protein. Also, the precipitated cells were resuspended with a PBS buffer and lysed by a micro tube mixer (MT-360, Tomy Seiko Co., Ltd., Tokyo, Japan) with glass beads (1.0 mm dia.). The cell lysis solution was centrifuged to obtain the cell-free extract. The expression of the fusion protein in both the culture broth supernatant and the cell-free extract was analyzed by SDS-PAGE and Western blot. The SDS–PAGE analysis was carried out with the supplier's protocol using Bolt™ 4–12% Bis-Tris Plus and MES SDS running buffer (Invitrogen, Carlsbad, CA, USA). The separated proteins were stained with Instant Blue™ (Expedeon, San Diego, CA, USA) or electroblotted to nitrocellulose membrane by Trans-Blot® Turbo™ transfer pack (Bio-Rad, Hercules, CA, USA) for the Western blot. After blocking with 5% (v/v) skim milk with 0.05% Tween/PBS (PBST), the membrane was washed three times with PBST for 10 min and incubated with a dilution of monoclonal mouse anti-His-tag antibody for 2 h, followed by washing. The membrane was incubated with a dilution of alkaline phosphatase (AP)-conjugated anti-mouse IgG as the secondary antibody and washed with the same procedure as followed above. The signal was detected with AP substrate by a colorimetric method.

2.4. Purification of Ex-(EBP)$_{10}$-6xHis by Ni–NTA affinity chromatography

The His-tagged fusion protein was purified by Ni–NTA affinity chromatography according to the manufacturer's instructions (Vunnum et al., 1998). Briefly, the Ni–NTA resin slurry was washed with distilled water and equilibrated with a binding buffer (1x Phosphate Buffered Saline (PBS), pH 7.4). The culture broth containing the fusion protein was loaded into the column and the flow-through fraction was collected. The weakly bound proteins were washed from the resin by a washing buffer (1x PBS at pH 7.4 containing 20 mM imidazole). The bound proteins were eluted with an elution buffer (1x PBS at pH 7.4 containing 250 mM imidazole). After purification, imidazole was removed using a dialysis tubular membrane (MWCO 3500 Da). The molecular weight of the purified Ex-(EBP)$_{10}$-6xHis was analyzed by MALDI-TOF to compare it with the theoretical molecular weight and to confirm that the N-terminus sequence integrity was maintained when it was secreted after the cleavage of the secretion peptide sequence.

2.5. HPLC analysis

The purified fusion protein was analyzed by a HPLC 1260 system (Agilent, Santa Clara, CA, USA) equipped with a size exclusion chromatography (SEC) column (Bio SEC-5 column, 150 Å, 5 μm; 4.6 mm ID) or a C18 reversed-phase column (Shim-pack GIS-ODS 5 μm; 250 × 4.6 mm ID, Dong-il Shimazu SpeChrom Corp., Seoul, Korea). For the SEC analysis, ca. 10 μg of the fusion protein was injected and analyzed for 45 min at 0.4 ml/min at 25°C using 1x PBS (pH 7.4) as the mobile phase. The eluent was monitored for the UV absorbance at 280 nm. The purity was determined by calculating the area % occupied by the fusion protein peak. The RP-HPLC (C18) analysis was performed at 25°C using a linear gradient of a hydrophilic solvent (buffer A; DW with 0.1% TFA) and a hydrophobic solvent (buffer B; acetonitrile with 0.1% TFA) at 0.6 ml/min. The elution times of Ex-(EBP)$_{10}$-6xHis and exenatide were compared to find any change in the hydrophobicity after EBPylation (Olsen, 2001).

2.6. cAMP assay for in vitro bioactivity analysis

To measure the bioactivity of the expressed fusion protein, we used a cAMP Hunter Exendin-4 Bioassay Kit from Discovery, Inc. (Fremont, CA, USA) using the engineered Chinese hamster ovary (CHO) cells with GLP-1 receptors expressed on their surfaces. When exenatide, a GLP-1 receptor agonist, binds to the GLP-1 receptor, the receptor modulates cAMP production by stimulating adenylate cyclase that is involved in a series of secondary messenger cascades. The receptor binding is monitored by measuring the cellular cAMP levels by competitive immunoassay based on Enzyme Fragment Complementation (EFC) technology. The bioactivity was calculated from the GLP-1 receptor binding level. *The cAMP assay we used involves the measurement of both receptor binding to the GLP-1 receptor and the subsequent intracellular signal transduction to produce cAMP. Thus, for the efficacy evaluation, cAMP assay is more comprehensive than SPR assay.* The half maximal effective concentration (EC_{50}) of the fusion protein was compared with that of native exenatide.

2.7. Physical half-life analysis by in vivo imaging system (IVIS)

All the mouse experiments were performed at the Center for Laboratory Animal Science at Hanyang University after the IRB approval complying with the Principles of Laboratory Animal Care of Hanyang University (No. 2017-0146). *In-vivo imaging is a direct and valid method widely employed to measure the bioavailability and biodistribution of a modified protein, including PEGylated proteins, by quantifying the residual fluorescence intensity* (Lee et al., 2014; Kim et al., 2011). The native exenatide and the purified Ex-(EBP)$_{10}$-6xHis were incubated with Flamma® 675 vinylsulfone (Ex/Em: 675/691 nm) fluorescent dye from Bioacts, Inc. (Incheon, Korea) in 50 mM borate buffer (molar ratio protein: dye = 1:5) for 24 h at 35°C. After the labeling reaction, the fluorescent dye-labeled protein and unreacted fluorescent dye were separated using a gel filtration column (PD MiniTrap G-25, GE Healthcare, Uppsala, Sweden). The labeled protein concentration and protein labeling ratio (dye/protein) were calculated with Eqs. (1) and (2) by measuring the absorbance of the labeled protein at 280 nm and 675 nm with a UV spectrometer.

$$\text{Concentration of labeled protein (M)} = \frac{[A_{280} - (A_{675} * CF_{280})]}{\varepsilon_{exenatide}} \quad (1)$$

Here, A_{280} and A_{675} are the absorbance of the labeled-protein at 280 nm and 675 nm, respectively. CF_{280} (correction factor for Flamma® 675 vinylsulfone), the absorbance of the fluorescent dye at 280 nm, is 0.09 and $\varepsilon_{exenatide}$, the molar absorption coefficient for exenatide is 5500 $cm^{-1}M^{-1}$. The protein labeling ratio is given by:

$$\text{protein labeling ratio (dye/protein)} = \frac{A_{675}}{\varepsilon_{dye} * \text{concentration of labeled protein } (M)} \quad (2)$$

Here, ε_{dye}, the molar absorption coefficient for dye, is 220,000 $cm^{-1}M^{-1}$.

The labeled proteins were diluted in 1x PBS to allow the injection of 20 μg of exenatide (final volume = 100 μl) into each mouse. The exenatide solution was administered subcutaneously to 5-week-old male BALB/c nude mice (8 mice, Orient Bio Inc., Seongnam, Korea) under anesthesia induced with 5% isoflurane. The fluorescence images of the mice were measured at 0, 1, 2, 4, 8, 12, 24, 48, 72, 96, and 147 h after injection using *in vivo* imaging system (IVIS® Luminar XR, Caliper Life Sciences, MA, USA) (Lee et al., 2014; Brom et al., 2012). In this experiment, the term 'physical half-life' was used to indicate how long fluorescence labeled drug substances stay in the body. The 'physical' half-life of the protein was measured by the fluorescence label intensity observed near the injection site and calculated by assuming the first-order kinetics of the fluorescence intensity elimination without considering the glucose-lowering bioactivity of the drug substances.

2.8. Intraperitoneal glucose tolerance test (IPGTT) and hypoglycemic test in vivo

To compare the *in vivo* biological potency and the biological half-life of the native exenatide and Ex-(EBP)$_{10}$-6xHis, IPGTT and hypoglycemic test were carried out in BKS.Cg-Dock7^{m}+/+Lepr^{db}/J mice (male, 5 week, Orient Bio Inc.) after 1-week adaptation to their environment before the experiment (IRB No. 2017-0233) (Han et al., 2014; Perez et al., 2013). Here, 'biological' half-life is determined by how long the glucose-lowering bioactivity of the drug substance is maintained *in vivo*. For the IPGTT, the drug substances were first injected subcutaneously (25 nmol/kg body weight) to the overnight-fasted mice, and at 1 h after the injection of the drug substance glucose solution (2 g/kg body weight) was administered intraperitoneally. Blood samples were drawn from the tail vein at 0, 20, 40 min, 1, 1.5, 2, 2.5, 3, and 4 h after the glucose administration to measure the blood glucose levels by using a blood glucose meter (SD CodeFree™, SD Biosensor Inc., Suwon, Korea). For the hypoglycemic test, the mice were allowed free access to food and water during the experiment and the drug substances were injected subcutaneously (25 nmol/kg body weight). Blood samples were drawn from the tail at 0, 20, 40 min, 1, 1.5, 2, 2.5, 3, 4, 8, and 12 h after the drug substance administration for blood glucose measurements. All the data were statistically analyzed by using Origin Pro® from Origin Lab Corporation©.

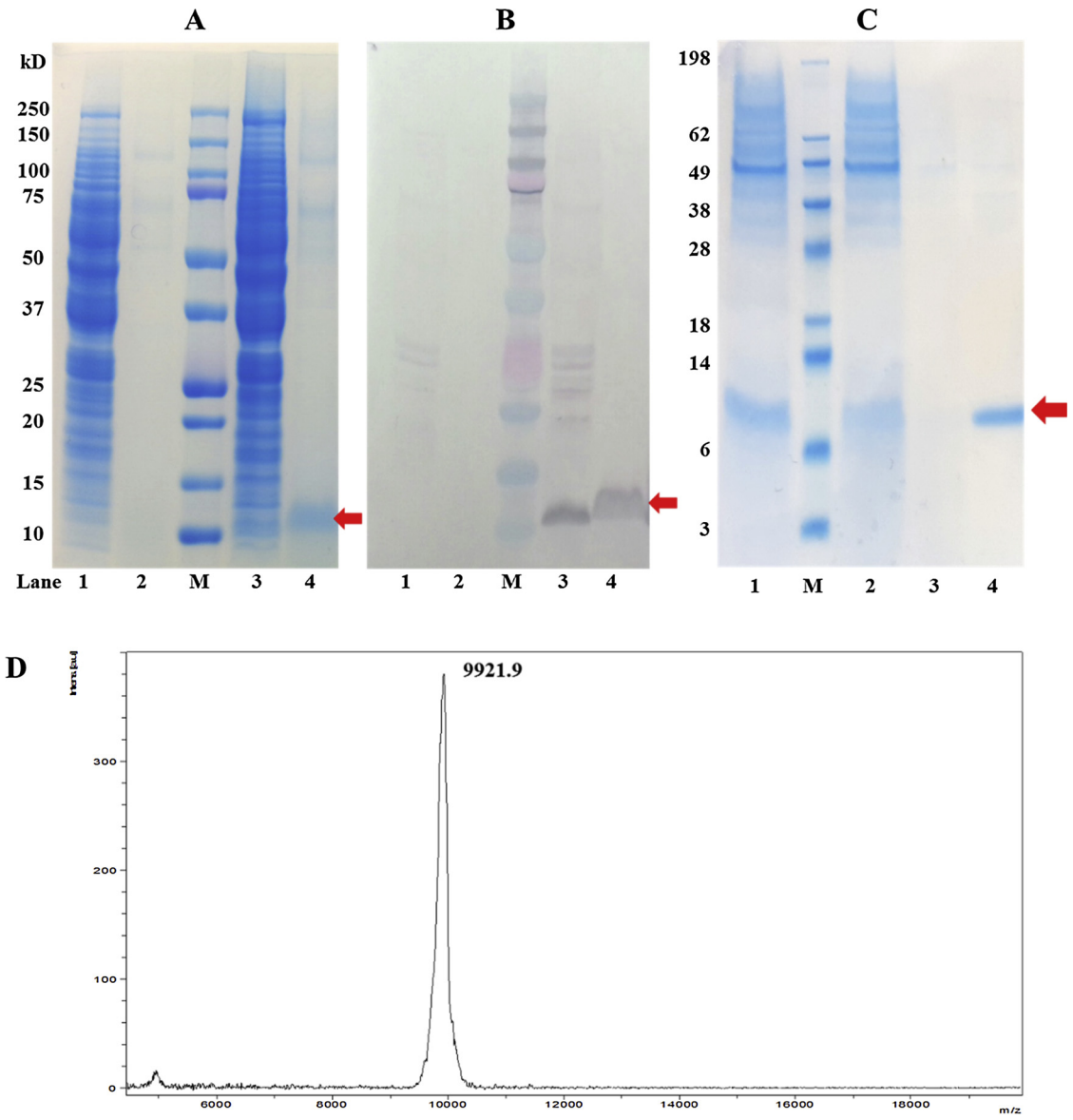

Fig. 1. Expression and purification of Ex-$(EBP)_{10}$-6xHis in *S. cerevisiae* Y2805.
Expression of Ex-$(EBP)_{10}$-6xHis analyzed by: (A) SDS-PAGE and (B) Western blot. Lane 1: Cell-free extract of non-transformed Y2805 (wild type); Lane 2: Culture broth supernatant of non-transformed Y2805; Lane 3: Cell-free extract of transformed Y2805 (Ex-$(EBP)_{10}$-6xHis); Lane 4: Culture broth supernatant of transformed Y2805 (Ex-$(EBP)_{10}$-6xHis).
(C) Purification of Ex-$(EBP)_{10}$-6xHis analyzed by SDS-PAGE. Lane 1: Culture broth (crude protein); Lane 2: Flow-through fraction from the Ni-NTA affinity column; Lane 3: Wash-out fraction from the column with 20 mM imidazole; Lane 4: Target protein (ca. 10 kD) eluted from the column with 250 mM imidazole. The position of the target protein is indicated by an arrow. (D) Molecular weight of the purified Ex-(EBP)10-6xHis analyzed by MALDI-TOF. The observed MW of the purified Ex-$(EBP)_{10}$-6xHis (9,921.9 Da) was in agreement with the theoretical MW (9,802.2 Da).

3. Results and discussion

3.1. Expression of Ex-$(EBP)_{10}$-6xHis

A recombinant *S. cerevisiae* strain containing the expression vector was cultivated in a galactose-containing medium (YPDG) for induced expression of the target gene. Fig. 1(A) and (B) shows the SDS-PAGE and Western blot results for the expression of the Ex-$(EBP)_{10}$-6xHis fusion protein in *S. cerevisiae*. A prominent band corresponding to approximately 10 kD (see lane 4, Fig. 1(A)) and a single major band (see lane 4, Fig. 1(B)), both in the culture broth supernatant of the transformed cells, were observed. Considering that no band was detected in both the cell-free extract and the culture broth supernatant of the non-transformed cells, we could conclude Ex-$(EBP)_{10}$-6xHis was successfully expressed in *S. cerevisiae* and secreted into the culture broth. It is interesting to note that the fusion proteins were also present inside the cells as evidenced by lane 3 in both SDS-PAGE and Western blot. However, in the case of yeast, the cell lysis process is complicated because of the thick cell wall, and too many endogenous proteins are present in the cell that makes it very difficult to purify the target protein after cell lysis. So, we decided to focus on purifying only the Ex-$(EBP)_{10}$-6xHis secreted to the broth.

Initially, we attempted an *E. coli* expression system to obtain Ex-$(EBP)_{10}$-6xHis fusion protein, but the expression level of the recombinant protein was extremely low under various induction conditions tested (data not shown). Fusion of the solubility-enhancing tags such as MBP (maltose binding protein), GST (glutathione S-transferase), or Trx (thioredoxin) resulted in a significantly improved expression level (data not shown) but the removal of the fusion tags required an additional costly process (Kapust and Waugh, 1999; Gopal and Kumar,

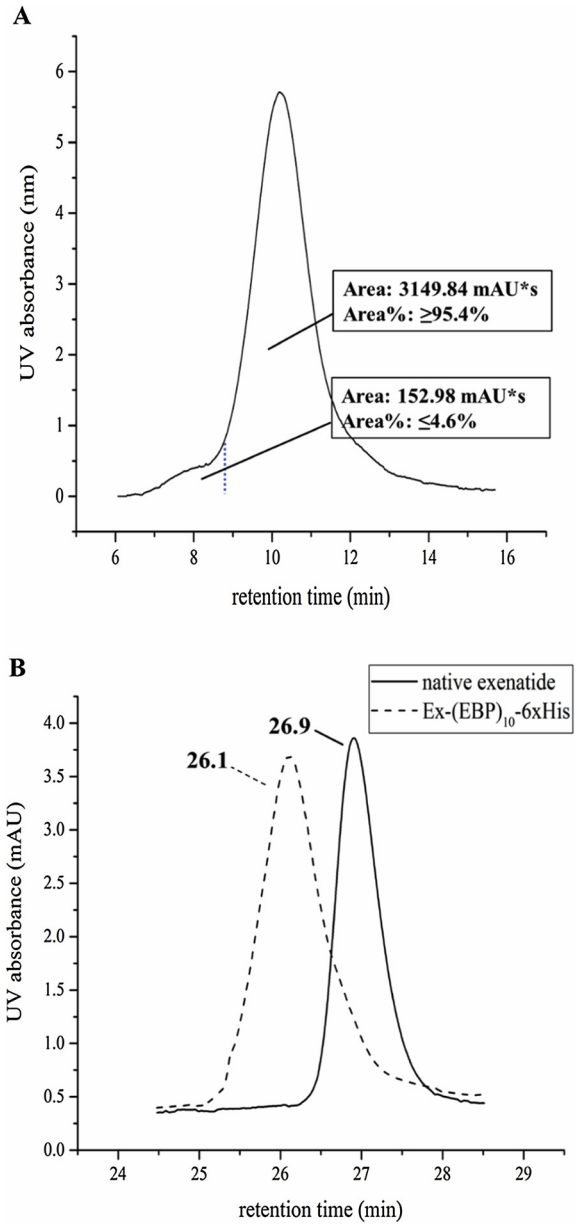

Fig. 2. SEC and RP-HPLC characterization of the purified Ex-$(EBP)_{10}$-6xHis. (A) The purity of Ex-$(EBP)_{10}$-6xHis was analyzed by SEC column (Bio SEC-5 Column 150 Å, 5 µm; 4.6 mm ID., Agilent, Santa Clara, CA, USA). About 10 µg of the fusion protein was injected and analyzed for 45 min at 0.4 ml/min using 1x PBS (pH 7.4) as the mobile phase (UV wavelength: 280 nm). When the two peaks were separated from each other at the boundary of 8.6 min in the program, the impurity peak area occupied 4.6% of the total peak area. Therefore, Ex-$(EBP)_{10}$-6xHis, which corresponds to the main peak, is estimated to occupy more than 95.4% of the area and thus show a purity of higher than 95%. (B) The hydrophilicity of protein was characterized using C18 column (Shim-pack GIS-ODS 5 µm; 250 × 4.6 mm ID., Dong-il Shimazu SpeChrom Corp., Seoul, Korea). The protein eluted by using a linear gradient of hydrophilic buffer (DW with 0.1% TFA) and hydrophobic buffer (acetonitrile with 0.1% TFA). Retention times of native exenatide (straight line) and Ex-$(EBP)_{10}$-6xHis (dash line) were 26.9 min and 26.1 min, respectively. Fusion with $(EBP)_{10}$ makes exenatide more hydrophilic than before.

2013; Marblestone et al., 2006). Intracellular expression also required the cell disruption to isolate the expressed protein. We also attempted a *Pichia pastoris* expression system to secrete the Ex-$(EBP)_{10}$-6xHis fusion protein, but it was not expressed at all (Jung, 2018). Therefore, we switched to the *S. cerevisiae* expression system for secretory expression. To the best of our knowledge, it is the first report that the galactose-induced *S. cerevisiae* system was employed to express the EBPylated exenatide.

3.2. Purification of Ex-$(EBP)_{10}$-6xHis by Ni–NTA affinity chromatography

Fig. 1(C) shows the SDS-PAGE result for the Ex-$(EBP)_{10}$-6xHis from culture broth supernatant purified by the Ni–NTA affinity chromatography. It confirmed that the fusion protein was neatly purified by the elution buffer (1x PBS buffer containing 250 mM imidazole). Although impurity bands with a molecular weight of 30 kD or more were observed, their concentrations were considerably lower than that of Ex-$(EBP)_{10}$-6xHis. After purification, imidazole was removed by dialysis and the concentration of the dialyzed protein was 0.06 mg/ml, which means that the *S. cerevisiae* expression system can produce ca. 18 mg of the purified protein from 1 L culture broth. It was reported that when exenatide was expressed and secreted in *Pichia pastoris*, ca. 150 mg exenatide was obtained from 1 L culture broth (Zhou et al., 2009). For exenatide fused with human serum albumin (HSA), with a total molecular weight of about 70 kD, ca. 73 mg fusion protein was produced from 1 L (Huang et al., 2008). Considering the MW difference between the 70 kD Ex-HSA and 10 kD Ex-$(EBP)_{10}$-6xHis, the yield from the *S. cerevisiae* system is at least comparable. *Also, compared with ca. 30–50 mg/L yield for the GLP-1 fused with a 50 kD ELP chain from E. coli expression, our yield (18 mg/L) was not lower on a molar basis. Considering the MW difference between the ca. 53 kD (theirs) and ca. 10 kD (ours), it is 0.6–1.0 mmol (theirs) vs. 1.8 mmol (ours). Furthermore, expression titer and purification yield are expected to improve after scale-up due to more precise process automation and control.*

Most of the EBPylation studies have focused on the changes of the phase transition property as a function of amino acid composition and repeat number of ELP. Also, ELPylated proteins have been purified using phase transition upon temperature change at a lab scale, where temperature changes are sharp and rapid; however, at a larger scale temperature changes can be slow, gradual, and not uniform inside a vessel. Another potential problem is the reversible nature of the phase transition: in large-scale centrifugation, it is difficult to maintain the uniform temperature from inlet to outlet from a centrifuge. That may be why in an industrial production of ELPylated GLP-1, temperature-dependent phase transition was not employed as a purification tool; instead, 3–4 chromatographic steps were used (Christiansen et al., 2013). *For a POC study with scale-up in our mind, we decided not to utilize the thermo-responsive property of the EBP for purification; instead, attached a poly-His tag at the C-terminus for affinity chromatography*.

3.3. MALDI-TOF mass spectrometry and N-terminus sequencing

Fig. 1(D) shows the MALDI-TOF mass spectrum showing the exact molecular weight of the purified Ex-$(EBP)_{10}$-6xHis. The molecular weight of the fusion protein was 9,921.9 Da, which is nearly the same as the theoretical molecular weight from its amino acid sequence (9,802.2 Da). The difference of 119.7 Da between the theoretical and the analytical value seems to be caused by insufficient desalting during the buffer exchange. When the fusion protein was secreted outside the cell, the MFα prepro secretion signal peptide is cleaved (Sohn et al., 1991; Kang et al., 1998). N-terminus sequencing analysis result confirmed that the N-terminus sequence of the secreted fusion protein was fully maintained without any loss (data not shown).

3.4. SEC and C18 RP-HPLC analysis

Fig. 2(A) shows the SEC chromatogram for the purified fusion protein as a single peak eluted at 10.2 min. However, a small shoulder peak was observed at ca. 8.5 min, which appears to be an impurity. These two peaks could hardly be separated due to the resolution limit of the column; however, the impurity peak accounted for only 4.6% of the

total peak area and, therefore, the purity was deemed higher than 95%. Fig. 2(B) shows the RP-HPLC chromatogram for the native exenatide (26.9 min retention time) and Ex-$(EBP)_{10}$-6xHis (26.1 min retention time, respectively, suggesting the hydrophilicity of Ex-$(EBP)_{10}$-6xHis had increased after the EBPylation. *It is interesting to see the EBPylate peak was eluted earlier than the unmodified one in RP-HPLC. It is something the theoretical prediction such as Gravy index on hydrophobicity did not match the experimental observation. It was also reported that aqueous solubility of GLP-1 was improved up to 50 mg/ml after ELP120 fusion, although the Gravy index was increased* (Christiansen et al., 2013). When PEG is attached to a peptide/protein, the conjugate's water solubility is improved because of the increased hydrophilicity, which in turn results in reduced aggregation and higher stability in long term storage (Knop et al., 2010). Based on this, we expect that the stability of Ex-$(EBP)_{10}$-6xHis be improved through increased hydrophilicity by attaching $(EBP)_{10}$ to the native exenatide.

3.5. cAMP assay (in vitro bioactivity analysis)

The insulin secretion activity of the native exenatide and Ex-$(EBP)_{10}$-6xHis was analyzed by cAMP assay (Zhang and Xie, 2012; Thomsen et al., 2005). Fig. 3 shows the result. The calculated EC_{50} of the native exenatide was 1.09 nM (R^2 = 0.969) and that of Ex-$(EBP)_{10}$-6xHis was 4.72 nM (R^2 = 0.992), which indicates that the fusion protein maintained approximately 72% of the bioactivity of the native form. The presence of an inert fusion partner domain is known to decrease the bioactivity of an active peptide/protein. For example, it was reported that, for mono-PEGylated interferon-α2a conjugated with various molecular weight PEGs, the interferon bioactivity decreased to 70.6, 55.3, and 21.3% of the native interferon for 5, 10, and 20 kD conjugated PEG, respectively (Lee et al., 2007). It may be far-fetched to compare the result directly; however, this result seems to indicate that the bioactivity may not be seriously deteriorated by the fused EBPs.

3.6. Physical Half-Life analysis by in vivo imaging system (IVIS)

The native exenatide and Ex-$(EBP)_{10}$-6xHis were labeled with Flamma® 675 vinylsulfone and subcutaneously injected into mice. The fluorescence intensity in the vicinity of the injection site was monitored

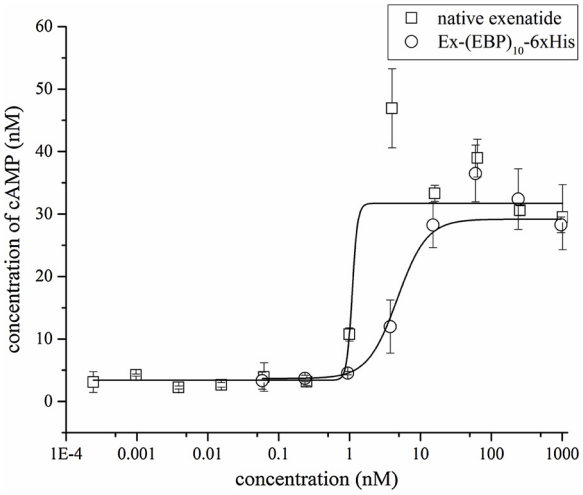

Fig. 3. Comparison of insulin secreting bioactivity by cAMP assay.
The cAMP assay (cAMP Hunter™ Exendin-4 Bioassay Kit, Discovery, Fremont, CA, USA) was used to measure cAMP concentration in CHO cell by GLP-1 receptor activation. The cAMP concentration is proportional to insulin secretion. Results are plotted as a mean ± SEM (n = 3) and fitted to a 4-parameter equation. The calculated EC_{50} of the native exenatide (□) was 1.09 nM (R^2 = 0.969) and the Ex-$(EBP)_{10}$-6xHis (○) was 4.72 nM (R^2 = 0.992), ca. 72% of the native form.

over time using the IVIS Living® (IVIS Imaging Program). Fig. 4 shows that the native exenatide rapidly distributed to the kidney, whereas Ex-$(EBP)_{10}$-6xHis maintained a relatively high fluorescence intensity near the injection site. *It is well known that EBPylation renders a thermo-responsive phase transition property to a protein, i.e., sol-like at a lower temperature and gel-like at a higher temperature. Thus, while the native exenatide could be distributed more readily to the kidney upon injection, a part of the EBPylated exenatide prepared at room temperature could change into a gel-like depot and be localized close to the injection site* (McDaniel et al., 2010). Fig. 5 shows the time-course changes in the fluorescence intensity near the injection site, after normalizing the intensity between the maximum value (100%) and the minimum value (0%). The intensity peaked at about 1 h after the injection, not immediately after the injection. This phenomenon was probably due to the hidden fluorescence that was not initially detected (Xie et al., 2017; Zhang et al., 2016).

In this experiment, the pharmacokinetics in the mouse body was easily evaluated by visualization but it was rather difficult to accurately determine the half-life due to the limitations of fluorescence detection from only the apparent tomography. Table 1 shows the change in the calculated fluorescence intensity at the injection site over time and the half-life ($t_{1/2}$) determined by applying the first-order elimination kinetics in Eq. (3) and the half-life formula in Eq. (4).

$$y(t) = Ae^{-kt} \tag{3}$$

$$t_{1/2} = \frac{ln\,2}{k} \tag{4}$$

Here, A is the initial concentration of the drug substance, k is the elimination rate constant, and $t_{1/2}$ is the half-life. When calculated, physical half-life of the native exenatide was 2.1 h (R^2 = 0.968) and that of the Ex-$(EBP)_{10}$-6xHis was 7.7 h (R^2 = 0.900); about a 3.7-fold longer half-life than the native exenatide. In another study, we found that when 5 kD PEG was conjugated to the same exenatide, its half-life was 2.2 h (R^2 = 0.966), about the same as that of the native exenatide (Nguyen et al., 2019). This result suggests that attaching $(EBP)_{10}$ instead of the PEG of the similar molecular weight (5 kD) might extend the physical half-life of the exenatide more effectively.

3.7. Intraperitoneal glucose tolerance test (IPGTT) and hypoglycemic test

Fig. 6 shows the time-course changes in the blood glucose level in the diabetic mice injected with native exenatide and Ex-$(EBP)_{10}$-6xHis (Kim et al., 2011; Qi et al., 2017). Fig. 6(A) shows the IPGTT result; both native exenatide and Ex-$(EBP)_{10}$-6xHis showed a stronger glucose tolerance than the PBS (control) group. *Biochemical analyte measurements of in-vivo samples from animal experiments may have larger error ranges than those from in-vitro lab experiments, so area under curve (AUC) analysis is frequently performed to assess a general trend during the test period. In our experiment, although the 4-h sample of PBS showed a lower glucose concentration than that of Ex-(EBP)10-6xHis, the AUC of the Ex-(EBP)10-6xHis showed almost a half of that of PBS.* The AUC of each curve would indicate the efficacy of the glucose-lowering bioactivity. For relative comparison, setting the AUC of the PBS control as 100%, native exenatide and Ex-$(EBP)_{10}$-6xHis showed 54.8% and 51.6%, respectively. Considering the mono-PEGylated exenatide (5 kD) showed 48.4% of AUC compared with the native exenatide in another study (Nguyen et al., 2019), we could conclude that both the EBPylated and PEGylated exenatide with the similar molecular weights demonstrated the similar glucose-lowering bioactivity *in-vivo*.

The hypoglycemic test was performed to measure the biological half-life that reflects the glucose lowering efficacy *in vivo*. In the hypoglycemic test, the blood glucose level initially decreased after a drug substance injection and then rebounded to the normal level. Fig. 6(B) shows the blood glucose level changes for the native exenatide and Ex-$(EBP)_{10}$-6xHis and the time required to reach the mean glucose level for

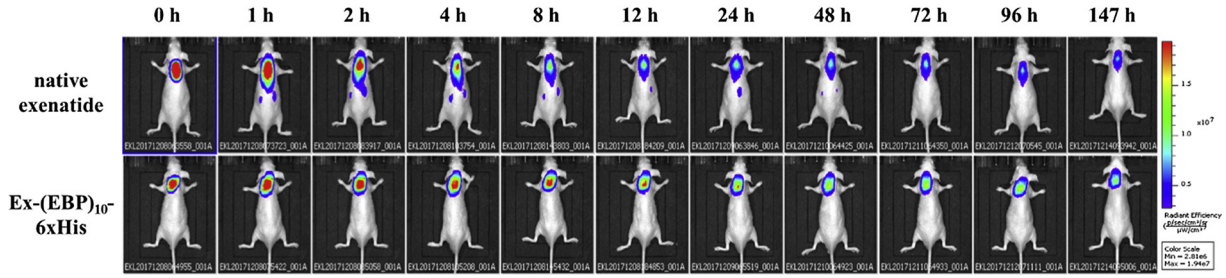

Fig. 4. Time-course monitoring of Flamma® 675 Vinylsulfone-tagged native exenatide and Ex-$(EBP)_{10}$-6xHis near the injection site of BALB/c nude mice after s.c. administration.
The Ex-$(EBP)_{10}$-6xHis maintained relatively high fluorescence intensity at the injection site; however the native exenatide reached to the kidney from the injection site faster due to rapid circulation over time.

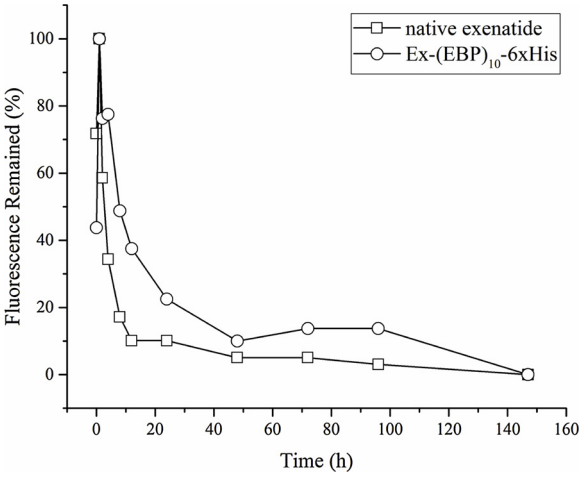

Fig. 5. Comparison of time-course profiles of fluorescence remained (%) of native exenatide and Ex-$(EBP)_{10}$-6xHis near the injection site of BALB/c nude mice.
The fluorescence intensity at the injection site of BALB/c nude mice was calculated and plotted with time, after setting the maximum value to 100% and the minimum value to 0%. The calculated physical half-life of the native exenatide (□) was 2.1 h (R^2 = 0.968) and the Ex-$(EBP)_{10}$-6xHis (○) was 7.7 h (R^2 = 0.900). Ex-$(EBP)_{10}$-6xHis showed about 3.7-fold higher half-life than the native exenatide.

the PBS treatment (ca. 500 mg/dL). The AUC of Ex-$(EBP)_{10}$-6xHis appears larger than that of the native exenatide; however, the time to return back to the control level was similar. *Biological half-life is a combined result of physical bioavailability (or stability) and in-vivo bioactivity. It means that, although physical half-life is increased by EBPylation, biological half-life could remain similar to that of a native protein due to the reduced in-vivo efficacy.* Considering the time to return back to the control level is proportional to the biological half-life, we can say that Ex-$(EBP)_{10}$-6xHis showed the similar biological half-life of ca. 8 h to the native exenatide, despite the 3.7-fold longer physical half-life. It is probably due to the reduced bioactivity; in other words, the extended physical half-life was offset by the reduced bioactivity (72% of the native form). However, mono-PEGylated (5 kD) exenatide that showed a similar biological half-life to that of the native exenatide maintained a much improved hypoglycemic bioactivity (Nguyen et al., 2019).

For a biobetter aimed at extending in-vivo half-life, we need to consider a balance between the extended half-life and reduced bioactivity (Zhai et al., 2009). *Very few data are available on the relationship between EBPylation chain length and bioactivity. In another study of our group, when the repeat number of EBP was 60, an exenatide analog's bioactivity was decreased to an approximately 50% level. When it was 120, the bioactivity dropped further to about 1/5* (Christiansen et al., 2013; Strohl, 2015). *It clearly indicates that as the EBP chain length increases the active domain's bioactivity decreases, just as in PEGylation.* The half-life will be further extended by using a higher repeat number of $(EBP)_n$ as a fusion domain; however, to maintain a required level of bioactivity it is necessary to find the optimal EBP repeat number. Future work will attempt to optimize the repeat number and parameterize the resulting bioactivity using the methodologies followed in this paper.

4. Conclusion

In this study, we have successfully produced a recombinant fusion protein, Ex-$(EBP)_{10}$-6xHis, from the galactose-induced *S. cerevisiae* expression system. The EBP domain contained 10 repeats of the pentapeptide with no linker sequence in between, a total of 50 amino acids. The fusion protein was expressed without promotor induction and secreted extracellularly. The protein was purified by Ni-NTA affinity chromatography to higher than 95% purity with an overall yield of ca. 18 mg per liter of the culture broth supernatant. This fusion protein showed an approximately 3.7-fold longer physical half-life in vivo while maintaining ca. 72% in-vitro bioactivity of the native exenatide. Mouse experiments revealed its biological half-life was similar to that of the native exenatide probably because the extended physical half-life was offset by the reduced bioactivity. While the effects of EBPylation on the fusion protein's bioactivity and half-life are similar to those of PEGylation, further study would focus on optimizing the EBP repeat number to maintain the required level of bioactivity. In summary, EBPylation can be an alternative half-life extension technology to PEGylation for improving patient convenience by reducing the injection frequency.

Table 1
Time-course profiles of fluorescence remained (%) and calculated physical half-life (h) of native exenatide and Ex-$(EBP)_{10}$-6xHis near the injection site of BALB/c nude mice.

Sample	Fluorescence Remained (%)											Physical Half-life (h)
	0 h	1 h	2 h	4 h	8 h	12 h	24 h	48 h	72 h	96 h	147 h	
Native exenatide	72	100	59	34	17	10	10	5	5	3	0	2.1
Ex-$(EBP)_{10}$-6xHis	44	100	76	78	49	38	23	10	14	14	0	7.7

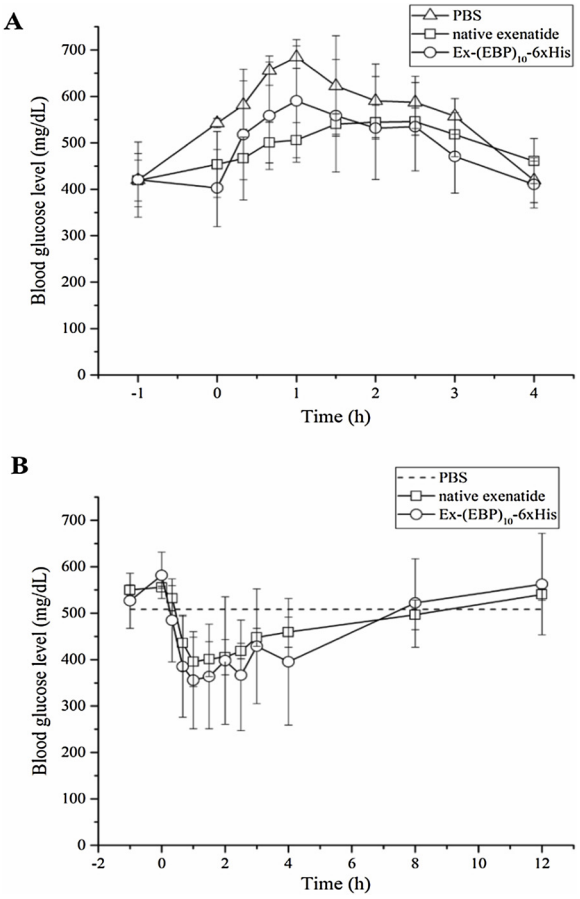

Fig. 6. In-vivo bioactivity and half-life analysis of native exenatide and Ex-$(EBP)_{10}$-6xHis by (A) IPGTT and (B) Hypoglycemic test.
The drug substances were injected (25 nmol/kg body weight) s.c. into BKS.Cg-Dock7^{m}+/+Lepr^{db}/J mice, and the blood glucose levels were measured at each time. Results are plotted as a mean ± SEM (n = 5). In IPGTT, the native exenatide (□) and the Ex-$(EBP)_{10}$-6xHis (○) show the similar glucose tolerance compared with the PBS (control) group. In hypoglycemic test, the calculated biological half-life of the native exenatide and Ex-$(EBP)_{10}$-6xHis were similar at ca. 8 h.

Acknowledgments

This work was supported by the National Research Foundation of Korea (NRF) Grant funded by the Korean Government (MSIP) (No. 2014R1A2A2A03004266).

References

Binder, U., Skerra, A., 2015. Current strategies for pharmacokinetic optimization. In: In: Rosenberg, A., Demeule, B. (Eds.), Biobetters, AAPS Advances in the Pharmaceutical Sciences Series, vol. 19. Springer, New York, pp. 269–311.
Brom, M., Joosten, L., Oyen, W.J., Gotthardt, M., Boerman, O.C., 2012. Radiolabelled GLP-1 analogues for in vivo targeting of insulinomas. Contrast Media Mol. Imaging 7, 160–166.
Bunck, M.C., Diamant, M., Cornér, A., Eliasson, B., Malloy, J.L., Shaginian, R.M., Deng, W., Kendall, D.M., Taskinen, M.-R., Smith, U., 2009. One-year treatment with exenatide improves β-cell function, compared with insulin glargine, in metformin-treated type 2 diabetic patients: a randomized, controlled trial. Diabetes Care 32, 762–768.
A. Chilkoti, Therapeutic agents comprising a GLP-1 receptor agonist and elastin-like peptide, U.S. Patent 8,178,495 (2012).
Choi, E.-S., Sohn, J.-H., Rhee, S.-K., 1994. Optimization of the expression system using galactose-inducible promoter for the production of anticoagulant hirudin in Saccharomyces cerevisiae. Appl. Microbiol. Biotechnol. 42, 587–594.
Christiansen, M., Matson, M., Brazg, R., 2013. Weekly subcutaneous doses of Glymera (PB1023), a novel GLP-1 analogue reduces glucose exposure dose dependently. Am. Diabetes Assoc. Abstr. 946P.
Chuang, V.T.G., Kragh-Hansen, U., Otagiri, M., 2002. Pharmaceutical strategies utilizing recombinant human serum albumin. Pharm. Res. 19, 569–577.
Eng, J., Kleinman, W., Singh, L., Singh, G., Raufman, J.-P., 1992. Isolation and characterization of exendin-4, an exendin-3 analogue, from Heloderma suspectum venom. Further evidence for an exendin receptor on dispersed acini from guinea pig pancreas. J. Biol. Chem. 267, 7402–7405.
Floss, D.M., Schallau, K., Rose-John, S., Conrad, U., Scheller, J., 2010. Elastin-like polypeptides revolutionize recombinant protein expression and their biomedical application. Trends Biotechnol. 28, 37–45.
Gopal, G.J., Kumar, A., 2013. Strategies for the production of recombinant protein in Escherichia coli. Protein J. 32, 419–425.
Han, J., Sun, L., Huang, X., Li, Z., Zhang, C., Qian, H., Huang, W., 2014. Novel coumarin modified GLP-1 derivatives with enhanced plasma stability and prolonged in vivo glucose-lowering ability. Br. J. Pharmacol. 171, 5252–5264.
Han, W., Chilkoti, A., López, G.P., 2017. Self-assembled hybrid elastin-like polypeptide/silica nanoparticles enable triggered drug release. Nanoscale 9, 6178–6186.
Harris, J.M., Chess, R.B., 2003. Effect of pegylation on pharmaceuticals. Nat. Rev. Drug Discov. 2, 214–221.
Hassouneh, W., MacEwan, S.R., Chilkoti, A., 2012. Fusions of elastin-like polypeptides to pharmaceutical proteins. Methods in Enzymology. Elsevier, pp. 215–237.
Hill, J., Donald, K.I.G., Griffiths, D.E., 1991. DMSO-enhanced whole cell yeast transformation. Nucleic Acids Res. 19 5791–5791.
Huang, Y.S., Chen, Z., Chen, Y.Q., Ma, G.C., Shan, J.F., Liu, W., Zhou, L.F., 2008. Preparation and characterization of a novel exendin-4 human serum albumin fusion protein expressed in Pichia pastoris. J. Pept. Sci. 14, 588–595.
Jung, S.J., 2018. Expression and Characterization of Exenatide and Elastin-Based Polypeptide Fusion Protein for Half-Life Extension. MS thesis. Department of Bionanotechnology, Graduate School Hanyang University, Ansan, Republic of Korea.
Kang, H.-A., Jung, M.-S., Hong, W.-K., Sohn, J.-H., Choi, E.-S., Rhee, S.-K., 1998. Expression and secretion of human serum albumin in the yeast Saccharomyces cerevisae. J. Microbiol. Biotechnol. 8, 42–48.
Kapust, R.B., Waugh, D.S., 1999. Escherichia coli maltose-binding protein is uncommonly effective at promoting the solubility of polypeptides to which it is fused. Protein Sci. 8, 1668–1674.
Kim, T.H., Jiang, H.H., Lee, S., Youn, Y.S., Park, C.W., Byun, Y., Chen, X., Lee, K.C., 2011. Mono-PEGylated dimeric exendin-4 as high receptor binding and long-acting conjugates for type 2 anti-diabetes therapeutics. Bioconjug. Chem. 22, 625–632.
Knop, K., Hoogenboom, R., Fischer, D., Schubert, U.S., 2010. Poly (ethylene glycol) in drug delivery: pros and cons as well as potential alternatives. Angew. Chemie Int. Ed. 49, 6288–6308.
Lee, B.K., Kwon, J.S., Kim, H.J., Yamamoto, S., Lee, E., 2007. Solid-phase PEGylation of recombinant interferon α-2a for site-specific modification: process performance, characterization, and in vitro bioactivity. Bioconjug. Chem. 18, 1728–1734.
Lee, C., Choi, J.S., Kim, I., Byeon, H.J., Kim, T.H., Oh, K.T., Lee, E.S., Lee, K.C., Youn, Y.S., 2014. Decanoic acid-modified glycol chitosan hydrogels containing tightly adsorbed palmityl-acylated exendin-4 as a long-acting sustained-release anti-diabetic system. Acta Biomater. 10, 812–820.
Marblestone, J.G., Edavettal, S.C., Lim, Y., Lim, P., Zuo, X., Butt, T.R., 2006. Comparison of SUMO fusion technology with traditional gene fusion systems: enhanced expression and solubility with SUMO. Protein Sci. 15, 182–189.
McDaniel, J.R., Callahan, D.J., Chilkoti, A., 2010. Drug delivery to solid tumors by elastin-like polypeptides. Adv. Drug Deliv. Rev. 62, 1456–1467.
Mentlein, R., Gallwitz, B., Schmidt, W.E., 1993. Dipeptidyl-peptidase IV hydrolyses gastric inhibitory polypeptide, glucagon-like peptide-1 (7–36) amide, peptide histidine methionine and is responsible for their degradation in human serum. FEBS J. 214, 829–835.
Nguyen, N.-T.T., Jung, S.J., Lim, D.W., Bae, O.N., Lee, E.K., 2019. Exenatide PEGylates in Various Configurations Show Enhanced Hypoglycemic Bioactivity and Extended In-vivo Half-Life. In preparation. .
Olsen, B.A., 2001. Hydrophilic interaction chromatography using amino and silica columns for the determination of polar pharmaceuticals and impurities. J. Chromatogr. A 913, 113–122.
Parkes, D., Jodka, C., Smith, P., Nayak, S., Rinehart, L., Gingerich, R., Chen, K., Young, A., 2001. Pharmacokinetic actions of exendin-4 in the rat: comparison with glucagon--like peptide-1. Drug Dev. Res. 53, 260–267.
Perez, J.R.T., Baritua, R.J., Pacalna, M.O., Malayao Jr, S.O., 2013. Exploratory investigation on the hypoglycemic effect of Abelmoschus esculentus in mice. Int. J. Sci. Technol. Res. 2, 249–253.
Podust, V.N., Balan, S., Sim, B.-C., Coyle, M.P., Ernst, U., Peters, R.T., Schellenberger, V., 2016. Extension of in vivo half-life of biologically active molecules by XTEN protein polymers. J. Control. Release 240, 52–66.
Qi, Y., Simakova, A., Ganson, N.J., Li, X., Luginbuhl, K.M., Ozer, I., Liu, W., Hershfield, M.S., Matyjaszewski, K., Chilkoti, A., 2017. A brush-polymer/exendin-4 conjugate reduces blood glucose levels for up to five days and eliminates poly (ethylene glycol) antigenicity. Nat. Biomed. Eng. 1, 0002.
Schellekens, H., Hennink, W.E., Brinks, V., 2013. The immunogenicity of polyethylene glycol: facts and fiction. Pharm. Res. 30, 1729–1734.
Sohn, J.-H., Lee, S.-K., Choi, E.-S., Rhee, S.-K., 1991. Gene expression and secretion of the anticoagulant hirudin in Saccharomyces cerevisiae. J. Microbiol. Biotechnol. 1, 266–273.
Strohl, W.R., 2015. Fusion proteins for half-life extension of biologics as a strategy to make biobetters. BioDrugs 29, 215–219.
Thomsen, W., Frazer, J., Unett, D., 2005. Functional assays for screening GPCR targets. Curr. Opin. Biotechnol. 16, 655–665.
Trabbic-Carlson, K., Liu, L., Kim, B., Chilkoti, A., 2004. Expression and purification of recombinant proteins from Escherichia coli: comparison of an elastin-like polypeptide fusion with an oligohistidine fusion. Protein Sci. 13, 3274–3284.

van Witteloostuijn, S.B., Pedersen, S.L., Jensen, K.J., 2016. Half-life extension of biopharmaceuticals using chemical methods: alternatives to PEGylation. ChemMedChem 11, 2474–2495.
Vunnum, S., Natarajan, V., Cramer, S., 1998. Immobilized metal affinity chromatography: self-sharpening of protein–modulator interfaces in frontal chromatography. J. Chromatogr. A 818, 31–41.
Waters, M.G., Evans, E.A., Blobel, G., 1988. Prepro-alpha-factor has a cleavable signal sequence. J. Biol. Chem. 263, 6209–6214.
Xie, C., Upputuri, P.K., Zhen, X., Pramanik, M., Pu, K., 2017. Self-quenched semiconducting polymer nanoparticles for amplified in vivo photoacoustic imaging. Biomaterials 119, 1–8.
Zhai, Y., Zhao, Y., Lei, J., Su, Z., Ma, G., 2009. Enhanced circulation half-life of site-specific PEGylated rhG-CSF: optimization of PEG molecular weight. J. Biotechnol. 142, 259–266.
Zhang, R., Xie, X., 2012. Tools for GPCR drug discovery. Acta Pharmacol. Sin. 33, 372–384.
Zhang, L., Wang, L., Meng, Z., Gan, H., Gu, R., Wu, Z., Gao, L., Zhu, X., Sun, W., Li, J., 2014. A novel exendin-4 human serum albumin fusion protein, E2HSA, with an extended half-life and good glucoregulatory effect in healthy rhesus monkeys. Biochem. Biophys. Res. Commun. 445, 511–516.
Zhang, D., Song, X.-j., Li, S.-y., Wang, S.-y., Chen, B.-j., Bai, X.-D., Tang, L.-m., 2016. Evaluation of liver function and electroacupuncture efficacy of animals with alcoholic liver injury by the novel imaging methods. Sci. Rep. 6.
Zhou, J., Cai, Z.-H., Li, L., Kou, C., Gao, Y.-F., 2009. Preparation and PEGylation of exendin-4 peptide secreted from yeast Pichia pastoris. Eur. J. Pharm. Biopharm. 72, 412–417.